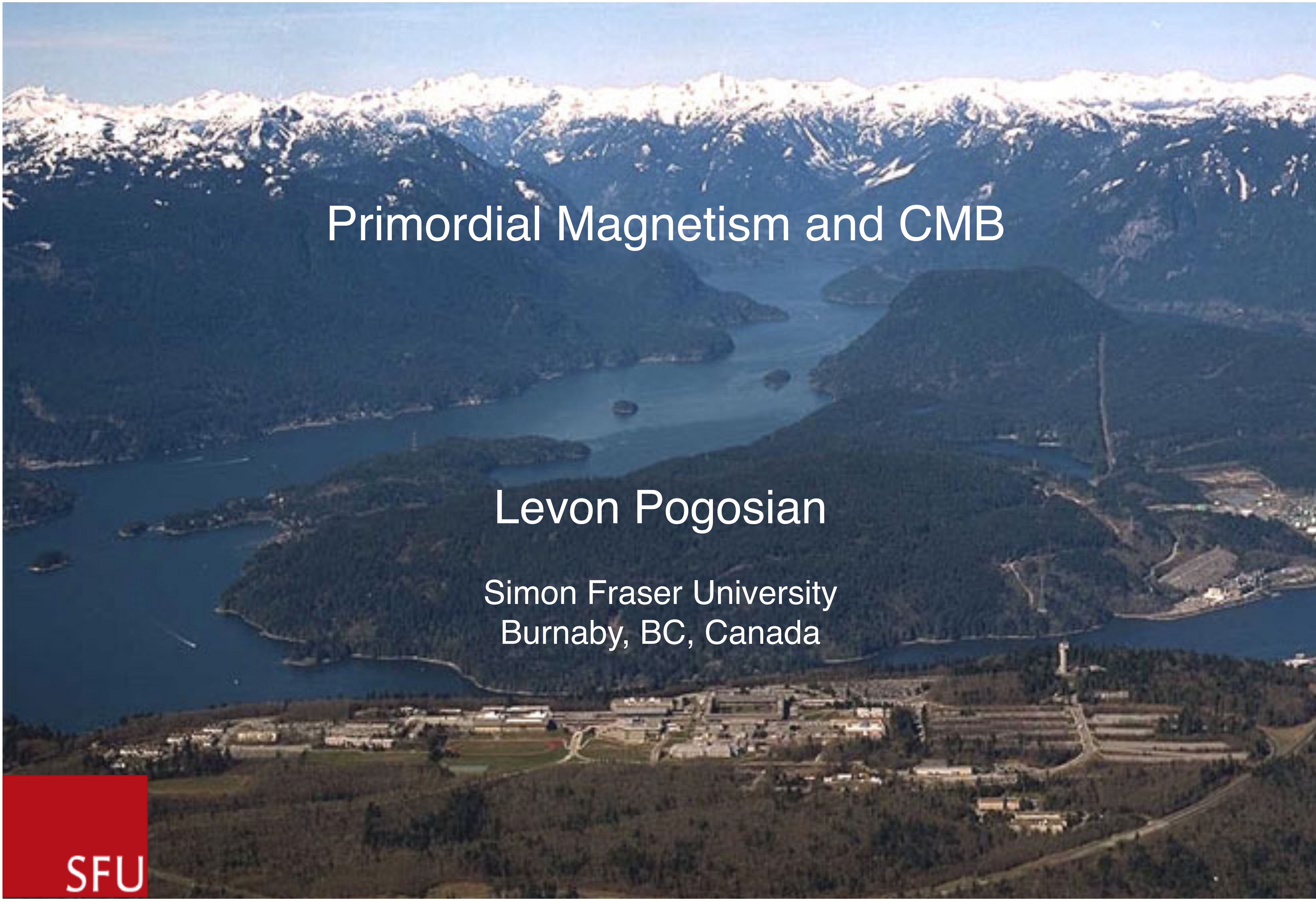

Primordial Magnetism and CMB

Levon Pogosian

Simon Fraser University
Burnaby, BC, Canada

SFU


SFU

16th Canadian Conference on General Relativity and Relativistic Astrophysics

6-8 July 2016, SFU Segal Building, Vancouver

Invited Speakers

Spyros Alexakis (Toronto)
† Robert Brandenberger (McGill)
Matt Choptuik (UBC)
David Garfinkle (Oakland)
Jack Gegenberg (New Brunswick)
Gil Holder (McGill)
Vicky Kaspi (McGill)
Luis Lehner (Perimeter)
† Don Page (Alberta)
Dejan Stojkovic (Buffalo)
† David Wands (Portsmouth)

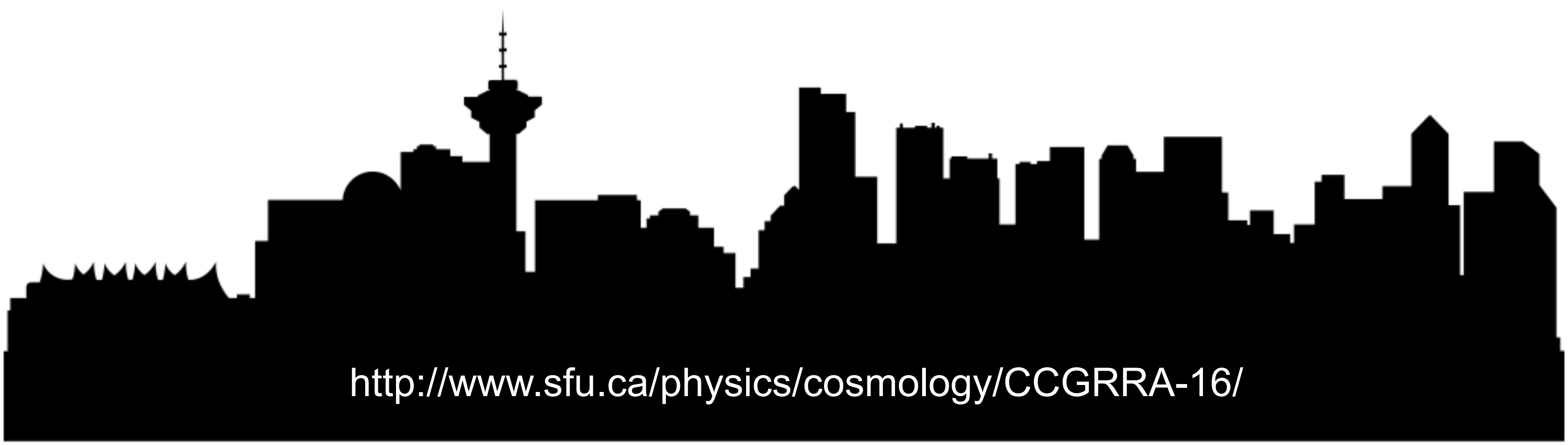

Primordial Magnetism and CMB

- Magnetic B-modes
- The promise of Faraday Rotation

Based on work with Soma De, Yun Li, Bess Ng, Tanmay Vachaspati, Amit Yadav, POLARBEAR collaboration

Cosmic Magnetic Fields

- Seen in galaxies and clusters
- Origin unknown
    - astrophysical?
    - primordial?
- Evidence (?) for intergalactic fields

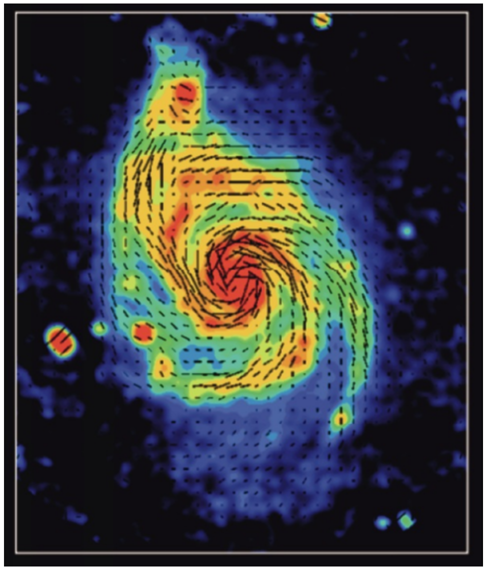

Image courtesy of NRAO/AUI

- Generated in the early universe – not "if", but "how much"
    - inflationary mechanism
    - phase transitions
    - a window into high energy physics and early universe
- A distinct CMB signature would prove their primordial origin

Magnetic field effects on CMB

- Gravitational coupling

$$T^0_0 \propto -B^2$$
$$T^i_j \propto B^2\delta^i_j - 2B^iB_j$$

scalar (curvature), vector (vorticity), tensor (gravity waves) modes

- Electromagnetic coupling

$$F_L = B \times (\nabla \times B)$$

Magnetic energy dissipates, dumps energy into the plasma

- spectral distortions
- modified ionization history

- Faraday Rotation

Stochastic Primordial Magnetic Field (PMF)

Magnetic field power spectrum:

$$\langle b_i(\mathbf{k}) b_j(\mathbf{k}') \rangle = (2\pi)^3 \delta^{(3)}(\mathbf{k} + \mathbf{k}')[(\delta_{ij} - \hat{k}_i \hat{k}_j) S(k) + i\varepsilon_{ijl} \hat{k}_l A(k)]$$

$$S(k) \propto k^n, \quad 0 < k < k_{\rm diss}$$

Common measures of cosmological magnetic fields:

$$B_\lambda^2 \equiv \int_0^\infty \frac{k^2 dk}{2\pi^2} S(k)\, e^{-\lambda^2 k^2} \qquad\qquad B_{\rm eff} \equiv \sqrt{8\pi\epsilon_B}$$

- Fields generated in phase transitions have n=2 for CMB-relevant k's
  (Durrer and Caprini, 2003; Jedamzik and Sigl, 2010)

- For scale-invariant PMF, n=-3: $B_\lambda = B_{\rm eff}$
  (Turner & Widrow, 1998; Ratra. 1992)

Observable CMB signatures of PMF

- Spatial correlations of anisotropies
- Shift in the time of last scattering
- Departures from the black body spectrum
- Faraday Rotation
  - Frequency dependence
  - Mode-coupling correlations

George Stokes
(1819–1903)

$$I = |E_x|^2 + |E_y|^2$$
$$Q = |E_x|^2 - |E_y|^2$$
$$U = 2\,\mathrm{Re}(E_x^* E_y)$$
$$V = 2\,\mathrm{Im}(E_x^* E_y)$$

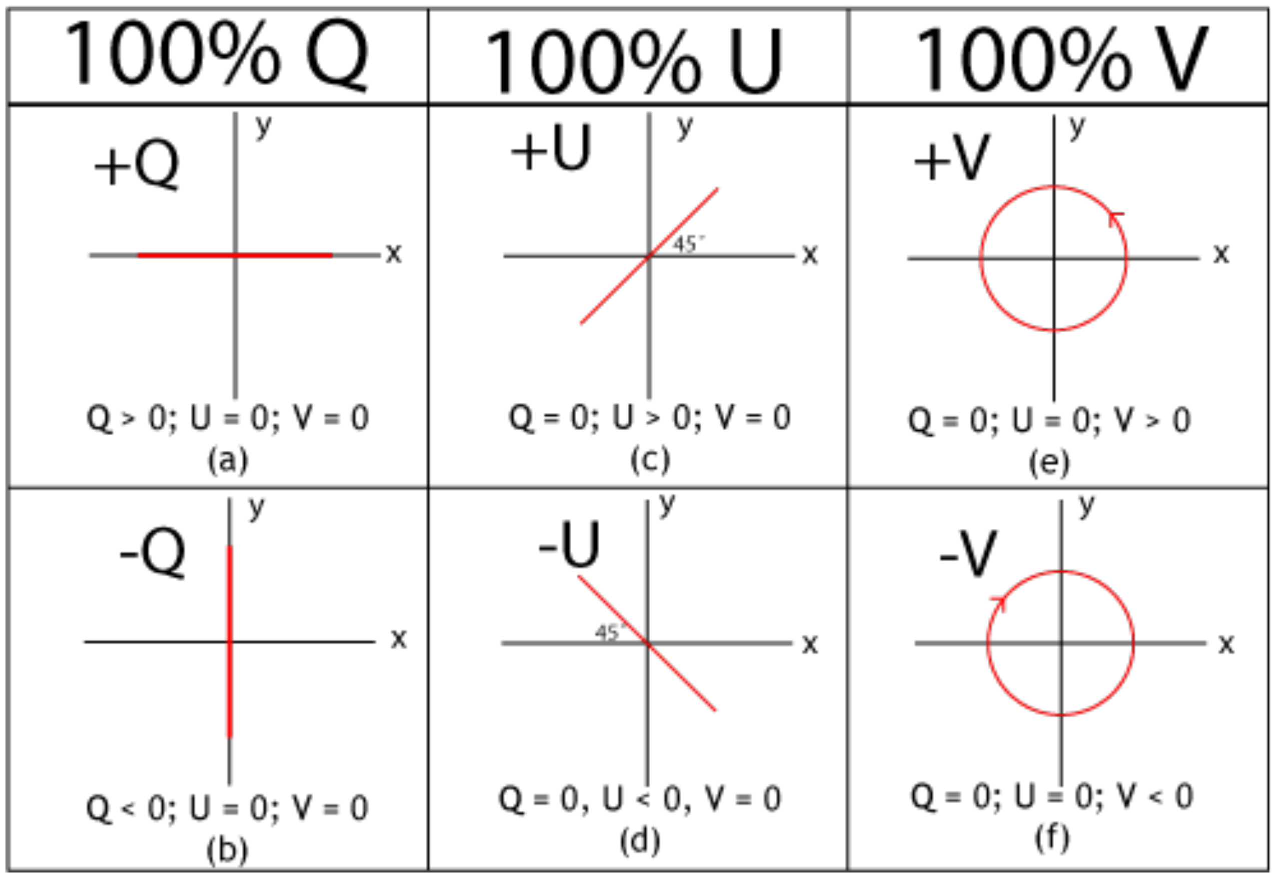

CMB Polarization

DASI

2002

$$P = \sqrt{Q^2 + U^2}$$

$$\alpha = \frac{1}{2}\arctan(U / Q)$$

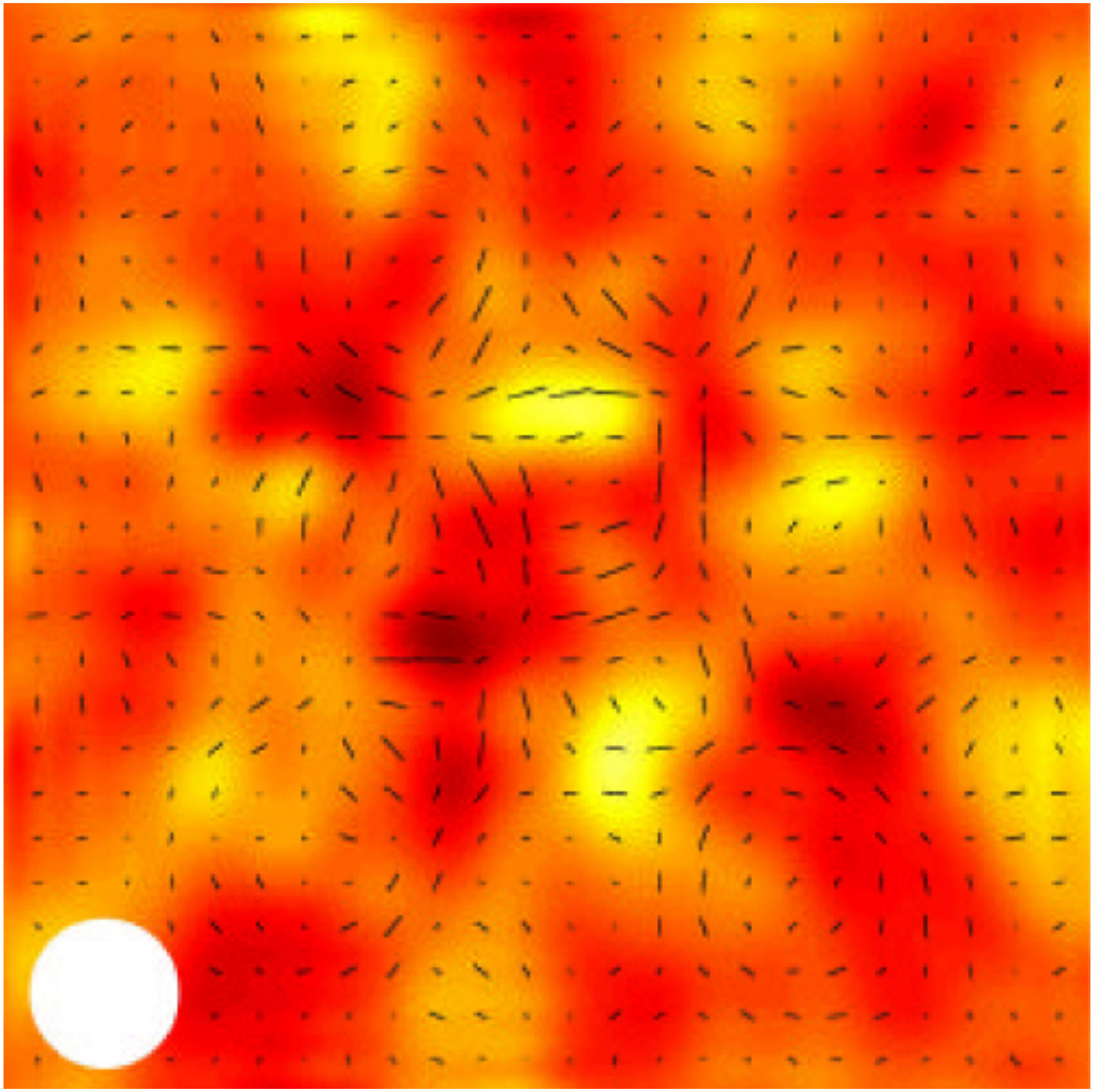

E (parity-even) and B (parity-odd) modes

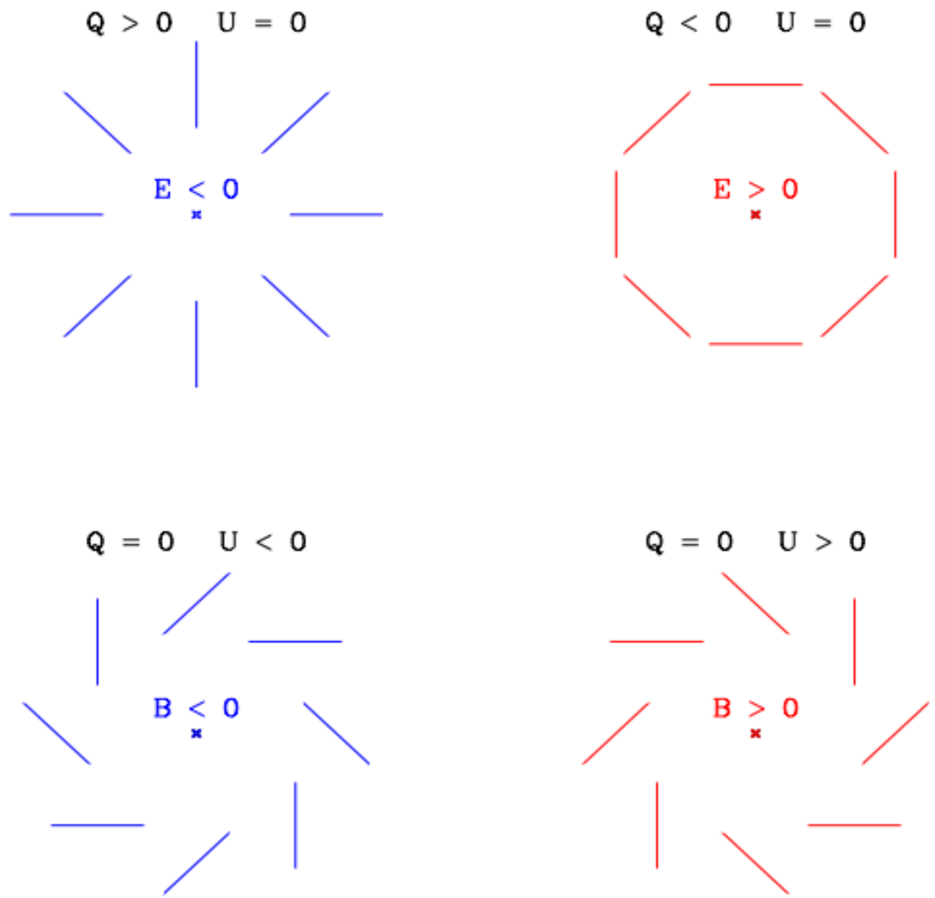

from M. Zaldarriaga, astro-ph/0305272

Shaw and Lewis
arXiv:0911.2714

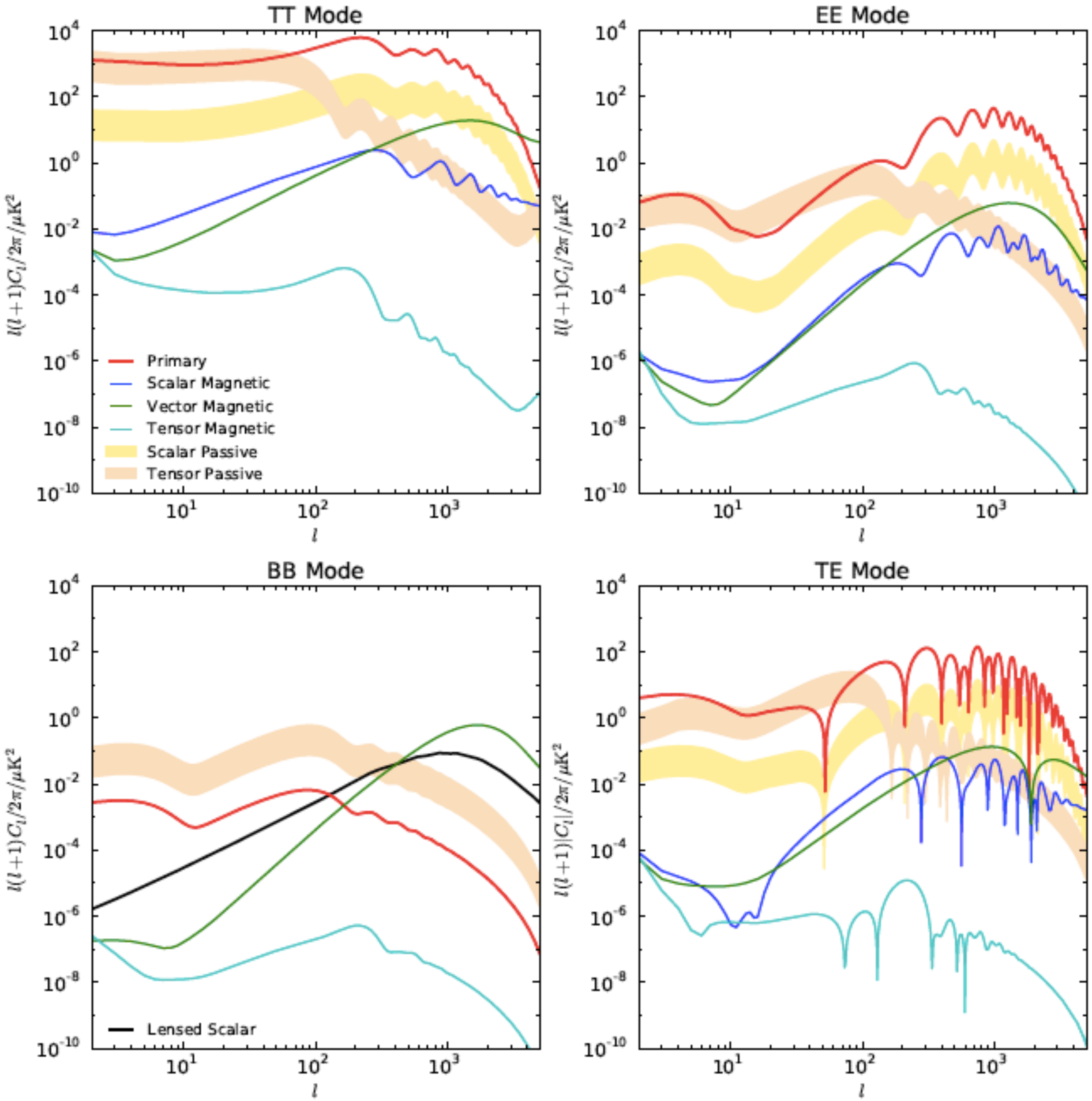

FIG. 2: The four CMB power spectra plotted for a realistic neutrino mass $\sum m_\nu = 0.47\,\mathrm{eV}$, with a magnetic field $B_\lambda = 4.7\,\mathrm{nG}$. We include the scalar primary contribution for the TT,EE and TE power spectra, and the tensor primary (with a tensor to scalar ratio of 0.1) and for the BB power spectrum. The shaded regions represent the regions we would expect the passive modes to lie within for production between the reheating and the electroweak transition.

B-modes from magnetic fields

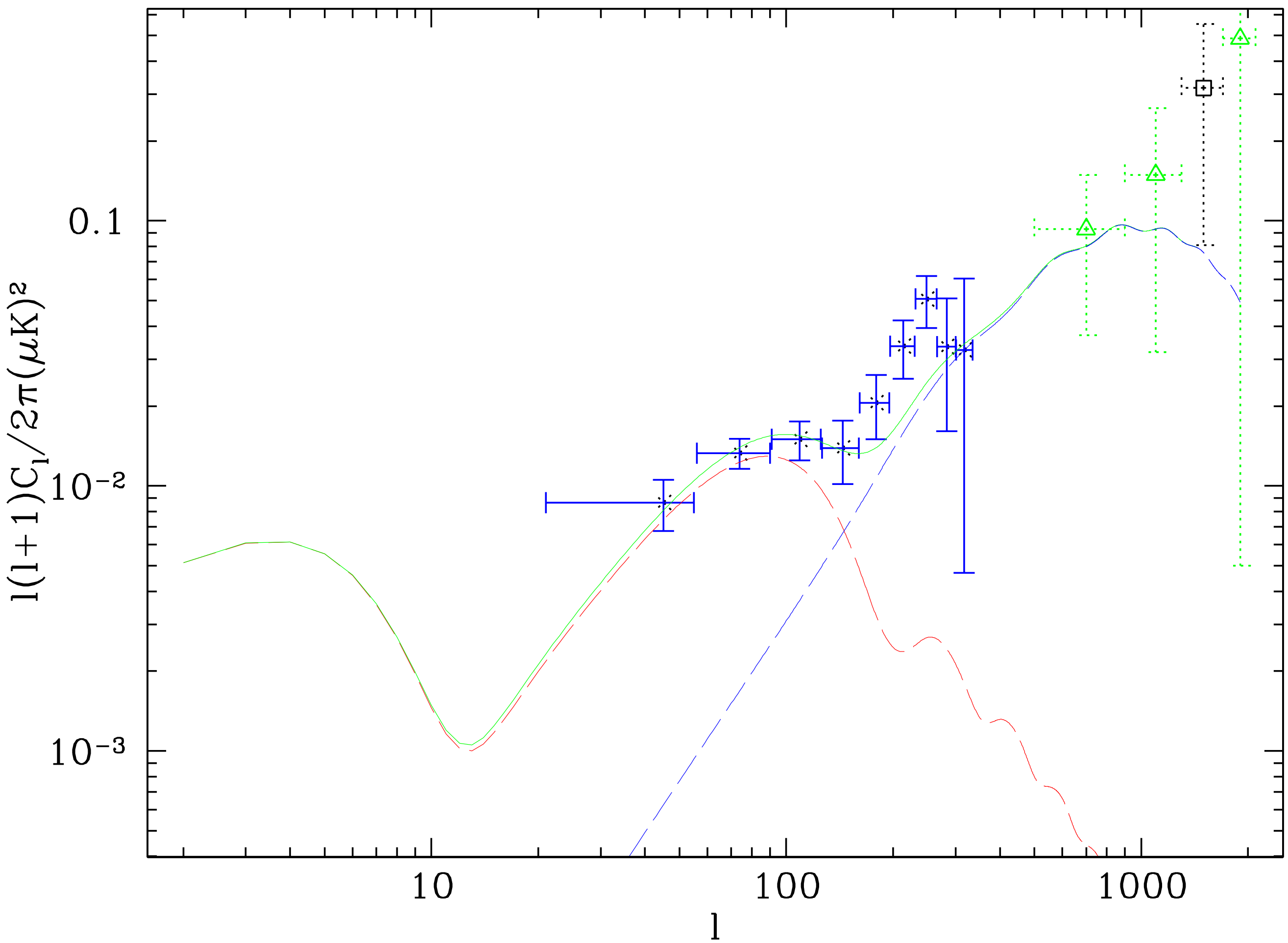

B-modes from magnetic fields

Bonvin, Durrer, Maartens, 1403.6768, PRL

$$B_1 = 1.83\,\mathrm{nG}, \quad T_* = 10^{14}\,\mathrm{GeV},$$
$$B_1 = 3.04\,\mathrm{nG}, \quad T_* = 10^{3}\,\mathrm{GeV},$$
$$B_1 = 5.5\,\mathrm{nG}, \quad T_* = 57\,\mathrm{MeV}.$$

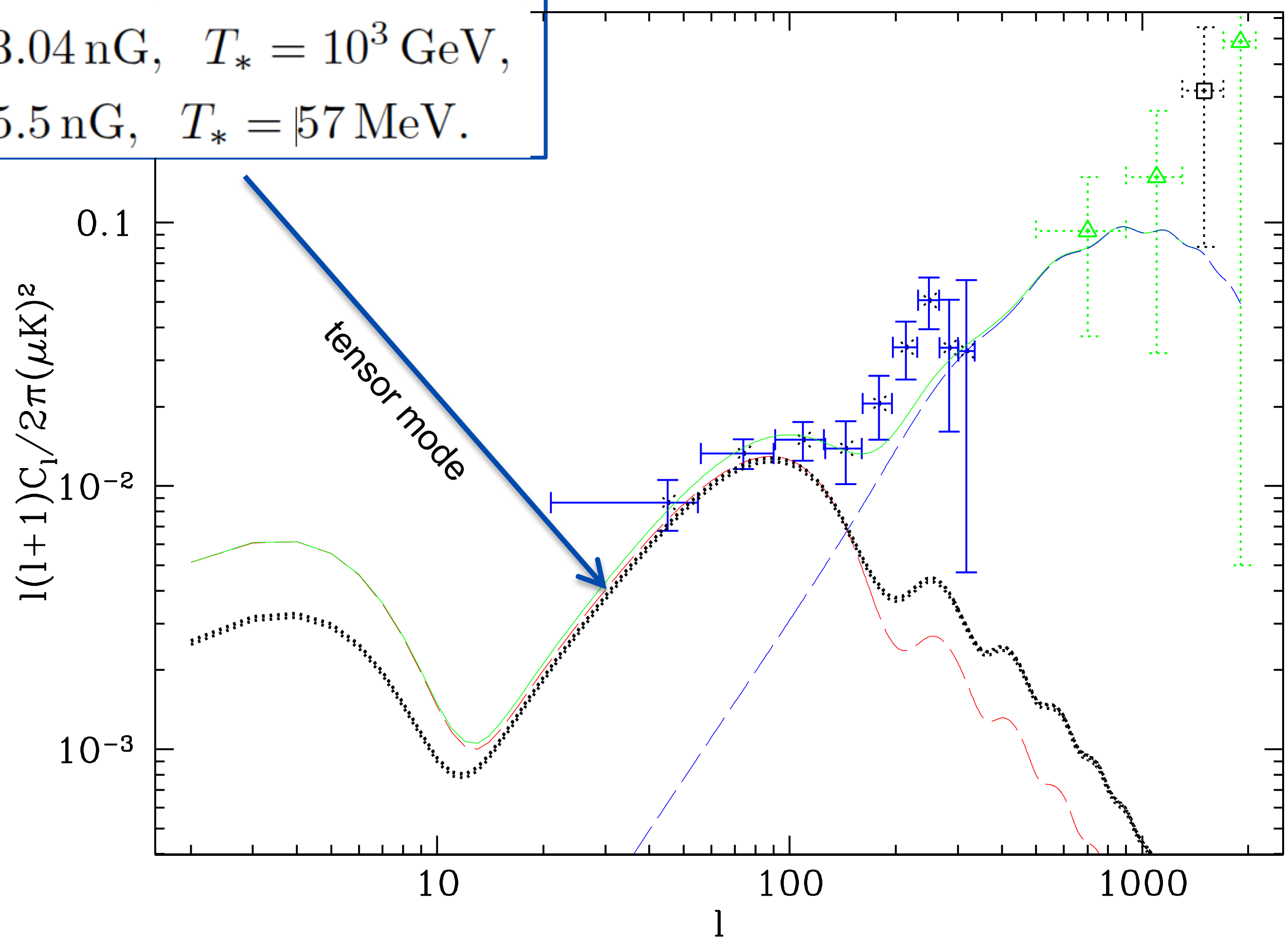

B-modes from magnetic fields

Bonvin, Durrer, Maartens, 1403.6768, PRL

$$B_1 = 1.83\,\mathrm{nG}, \quad T_* = 10^{14}\,\mathrm{GeV},$$
$$B_1 = 3.04\,\mathrm{nG}, \quad T_* = 10^{3}\,\mathrm{GeV},$$
$$B_1 = 5.5\,\mathrm{nG}, \quad T_* = 57\,\mathrm{MeV}.$$

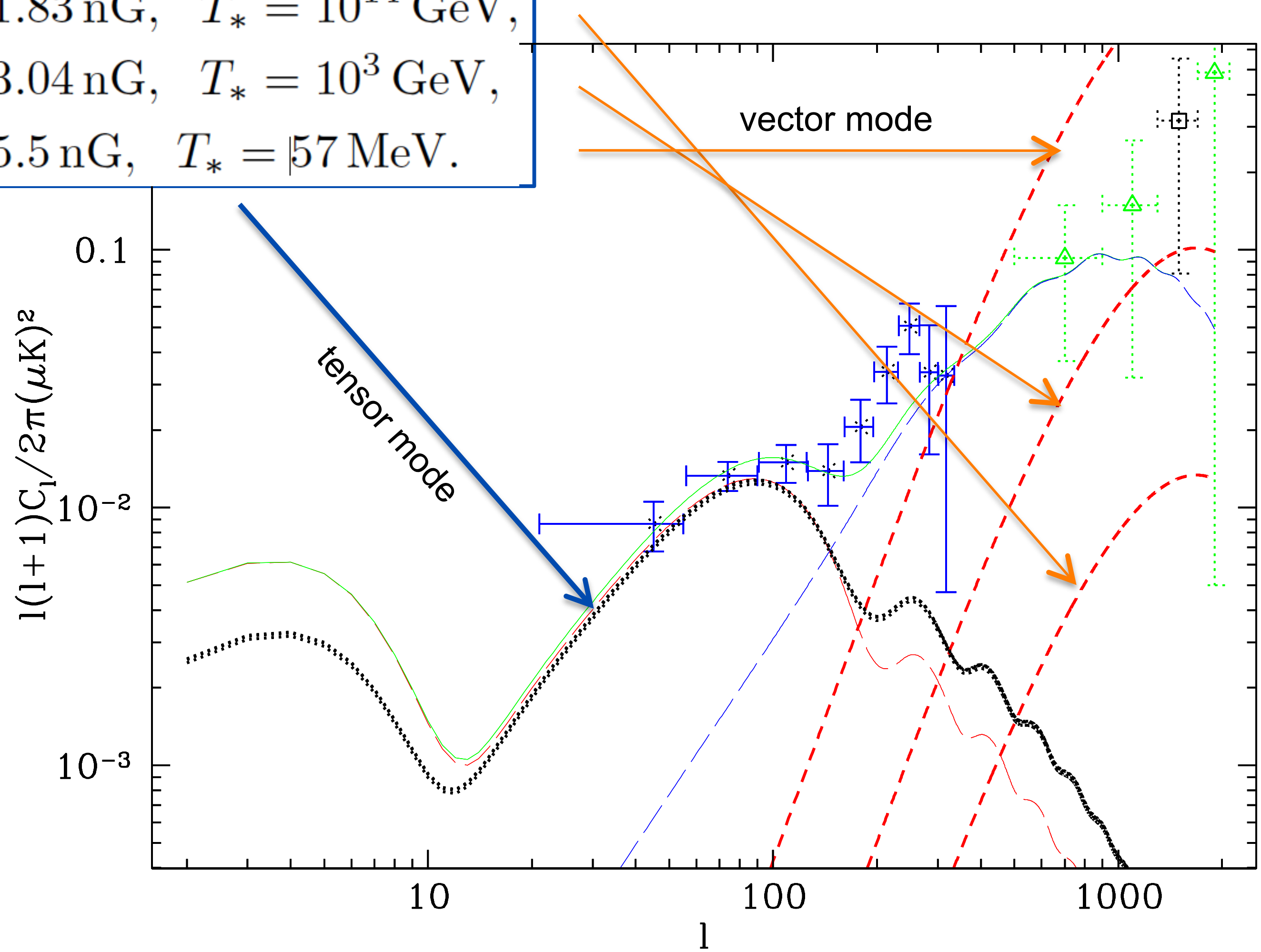

B-modes from magnetic fields

Bonvin, Durrer, Maartens, 1403.6768, PRL

$$B_1 = 1.83\,\mathrm{nG}, \quad T_* = 10^{14}\,\mathrm{GeV},$$
$$B_1 = 3.04\,\mathrm{nG}, \quad T_* = 10^{3}\,\mathrm{GeV},$$
$$B_1 = 5.5\,\mathrm{nG}, \quad T_* = 57\,\mathrm{MeV}.$$

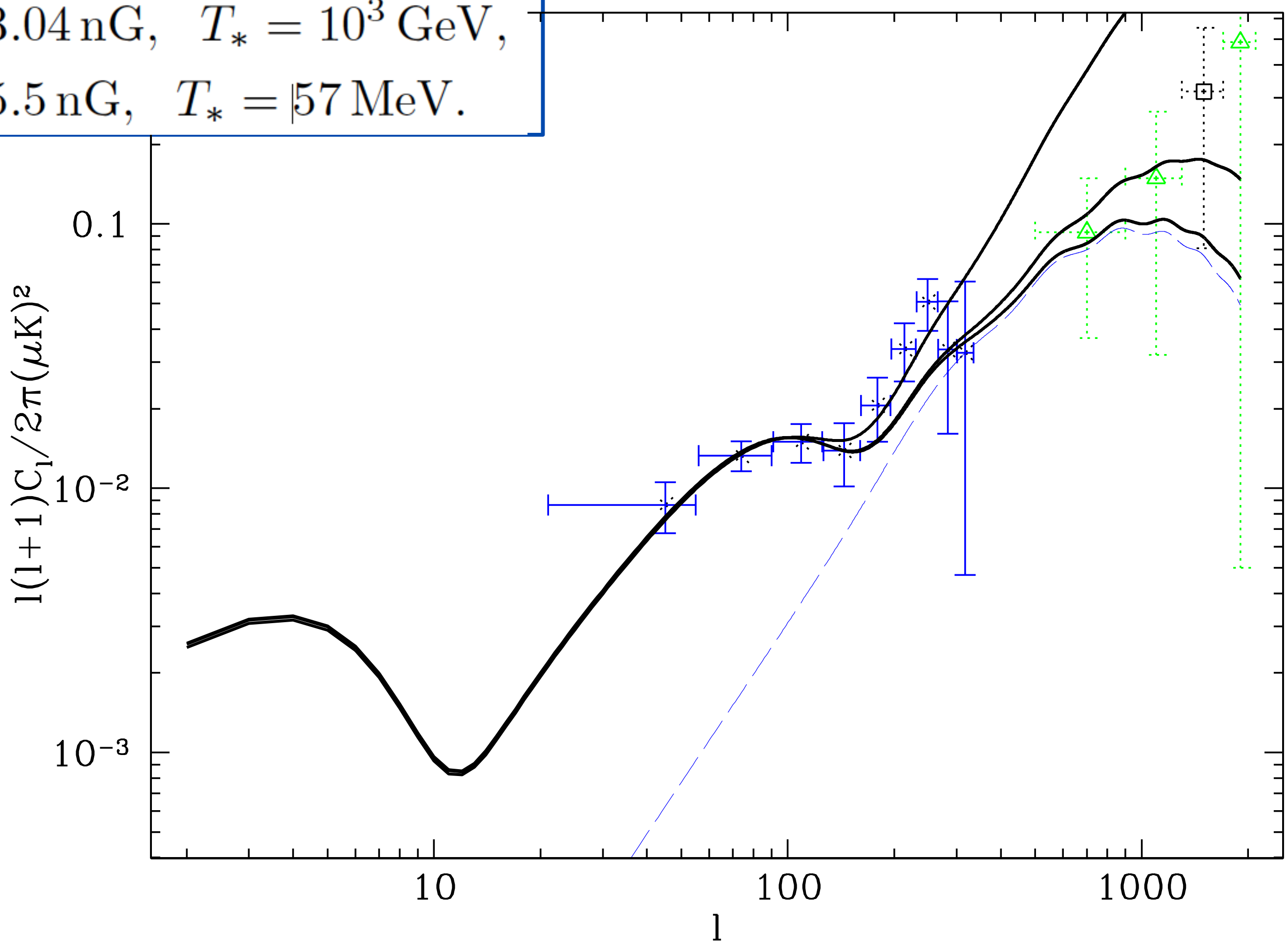

Planck 2015 results. XIX. Constraints on primordial magnetic fields

Planck Collaboration: P. A. R. Ade[91], N. Aghanim[63], M. Arnaud[77], F. Arroja[70,83], M. Ashdown[73,6], J. Aumont[63], C. Baccigalupi[90], M. Ballardini[51,53,32], A. J. Banday[101,9], R. B. Barreiro[69], N. Bartolo[31,70], E. Battaner[103,104], K. Benabed[64,100], A. Benoît[61], A. Benoit-Lévy[25,64,100], J.-P. Bernard[101,9], M. Bersanelli[35,52], P. Bielewicz[101,9,90], A. Bonaldi[72], L. Bonavera[69], J. R. Bond[8], J. Borrill[14,95], F. R. Bouchet[64,93], M. Bucher[1], C. Burigana[51,33,53], R. C. Butler[51], E. Calabrese[98], J.-F. Cardoso[78,1,64], A. Catalano[79,76], A. Chamballu[77,16,63], H. C. Chiang[28,7], J. Chluba[24,73], P. R. Christensen[87,39], S. Church[97], D. L. Clements[59], S. Colombi[64,100], L. P. L. Colombo[23,71], C. Combet[79], F. Couchot[74], A. Coulais[76], B. P. Crill[71,11], A. Curto[6,69], F. Cuttaia[51], L. Danese[90], R. D. Davies[72], R. J. Davis[72], P. de Bernardis[34], A. de Rosa[51], G. de Zotti[48,90], J. Delabrouille[1], F.-X. Désert[57], J. M. Diego[69], K. Dolag[102,84], H. Dole[63,62], S. Donzelli[52], O. Doré[71,11], M. Douspis[63], A. Ducout[64,59], X. Dupac[41], G. Efstathiou[66], F. Elsner[25,64,100], T. A. Enßlin[84], H. K. Eriksen[67], J. Fergusson[12], F. Finelli[51,53], E. Florido[103], O. Forni[101,9], M. Frailis[50], A. A. Fraisse[28], E. Franceschi[51], A. Frejsel[87], S. Galeotta[50], S. Galli[64], K. Ganga[1], M. Giard[101,9], Y. Giraud-Héraud[1], E. Gjerløw[67], J. González-Nuevo[69,90], K. M. Górski[71,105], S. Gratton[73,66], A. Gregorio[36,50,56], A. Gruppuso[51], J. E. Gudmundsson[28], F. K. Hansen[67], D. Hanson[85,71,8], D. L. Harrison[66,73], G. Helou[11], S. Henrot-Versillé[74], C. Hernández-Monteagudo[13,84], D. Herranz[69], S. R. Hildebrandt[71,11], E. Hivon[64,100], M. Hobson[6], W. A. Holmes[71], A. Hornstrup[17], W. Hovest[84], K. M. Huffenberger[26], G. Hurier[63], A. H. Jaffe[59], T. R. Jaffe[101,9], W. C. Jones[28], M. Juvela[27], E. Keihänen[27], R. Keskitalo[14], J. Kim[84], T. S. Kisner[81], J. Knoche[84], M. Kunz[18,63,3], H. Kurki-Suonio[27,46], G. Lagache[5,63], A. Lähteenmäki[2,46], J.-M. Lamarre[76], A. Lasenby[6,73], M. Lattanzi[33], C. R. Lawrence[71], J. P. Leahy[72], R. Leonardi[41], J. Lesgourgues[99,89,75], F. Levrier[76], M. Liguori[31,70], P. B. Lilje[67], M. Linden-Vørnle[17], M. López-Caniego[41,69], P. M. Lubin[29], J. F. Macías-Pérez[79], G. Maggio[50], D. Maino[35,52], N. Mandolesi[51,33], A. Mangilli[63,74], P. G. Martin[8], E. Martínez-González[69], S. Masi[34], S. Matarrese[31,70,44], P. Mazzotta[37], P. McGehee[60], P. R. Meinhold[29], A. Melchiorri[34,54], L. Mendes[41], A. Mennella[35,52], M. Migliaccio[66,73], S. Mitra[58,71], M.-A. Miville-Deschênes[63,8], D. Molinari[69,51], A. Moneti[64], L. Montier[101,9], G. Morgante[51], D. Mortlock[59], A. Moss[92], D. Munshi[91], J. A. Murphy[86], P. Naselsky[87,39], F. Nati[28], P. Natoli[33,4,51], C. B. Netterfield[20], H. U. Nørgaard-Nielsen[17], F. Noviello[72], D. Novikov[82], I. Novikov[87,82], N. Oppermann[8], C. A. Oxborrow[17], F. Paci[90], L. Pagano[34,54], F. Pajot[63], D. Paoletti[51,53,⋆], F. Pasian[50], G. Patanchon[1], O. Perdereau[74], L. Perotto[79], F. Perrotta[90], V. Pettorino[45], F. Piacentini[34], M. Piat[1], E. Pierpaoli[23], D. Pietrobon[71], S. Plaszczynski[74], E. Pointecouteau[101,9], G. Polenta[4,49], L. Popa[65], G. W. Pratt[77], G. Prézeau[11,71], S. Prunet[64,100], J.-L. Puget[63], J. P. Rachen[21,84], R. Rebolo[68,15,40], M. Reinecke[84], M. Remazeilles[72,63,1], C. Renault[79], A. Renzi[38,55], I. Ristorcelli[101,9], G. Rocha[71,11], C. Rosset[1], M. Rossetti[35,52], G. Roudier[1,76,71], J. A. Rubiño-Martín[68,40], B. Ruiz-Granados[103], B. Rusholme[60], M. Sandri[51], D. Santos[79], M. Savelainen[27,46], G. Savini[88], D. Scott[22], M. D. Seiffert[71,11], E. P. S. Shellard[12], M. Shiraishi[31,70], L. D. Spencer[91], V. Stolyarov[6,73,96], R. Stompor[1], R. Sudiwala[91], R. Sunyaev[84,94], D. Sutton[66,73], A.-S. Suur-Uski[27,46], J.-F. Sygnet[64], J. A. Tauber[42], L. Terenzi[43,51], L. Toffolatti[19,69,51], M. Tomasi[35,52], M. Tristram[74], M. Tucci[18], J. Tuovinen[10], G. Umana[47], L. Valenziano[51], J. Valiviita[27,46], B. Van Tent[80], P. Vielva[69], F. Villa[51], L. A. Wade[71], B. D. Wandelt[64,100,30], I. K. Wehus[71], D. Yvon[16], A. Zacchei[50], and A. Zonca[29]

(Affiliations can be found after the references)

Preprint online version: February 5, 2015

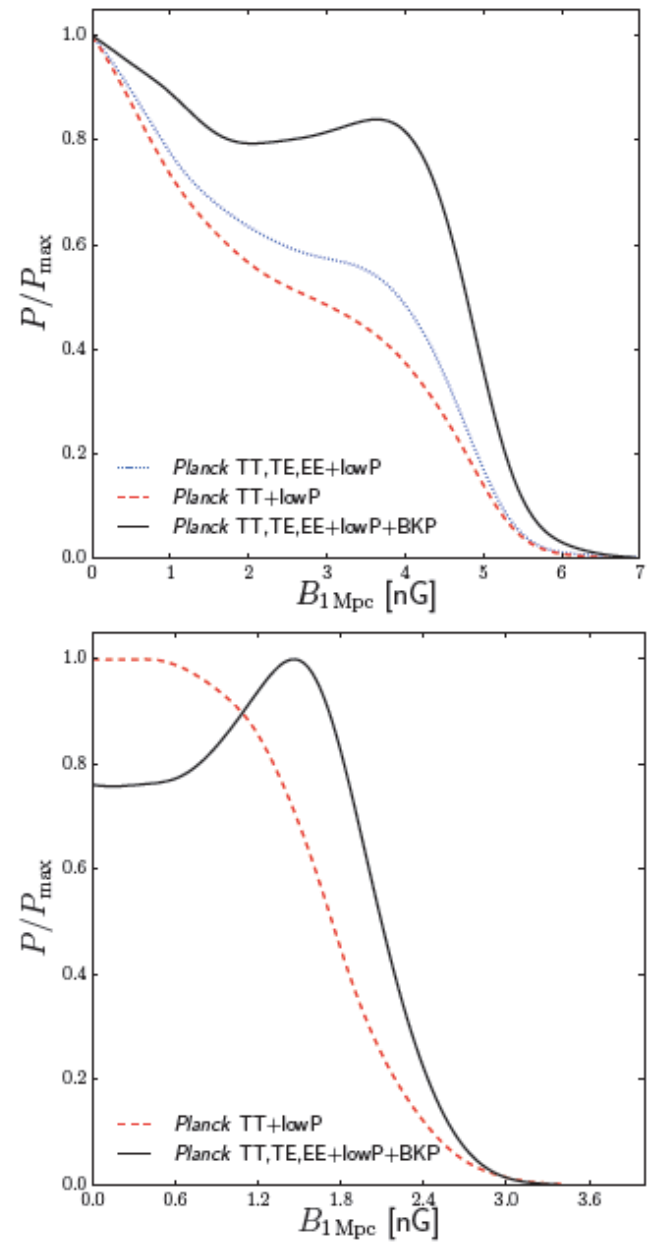

Fig. 11. Probability distributions for the PMF amplitude including the BICEP2/*Keck-Planck* cross-correlation, compared with the one based only on *Planck* data. *Top*: the case in which the spectral index is free to vary, *bottom*: the case with $n_B = -2.9$.

POLARBEAR Constraints on Cosmic Birefringence and Primordial Magnetic Fields

arXiv:1509.02461, Phys Rev D

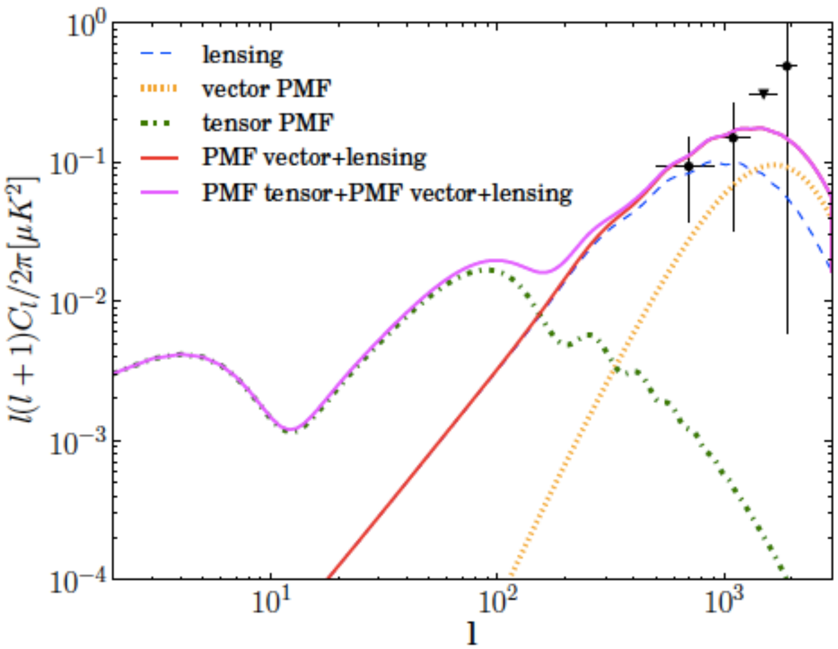

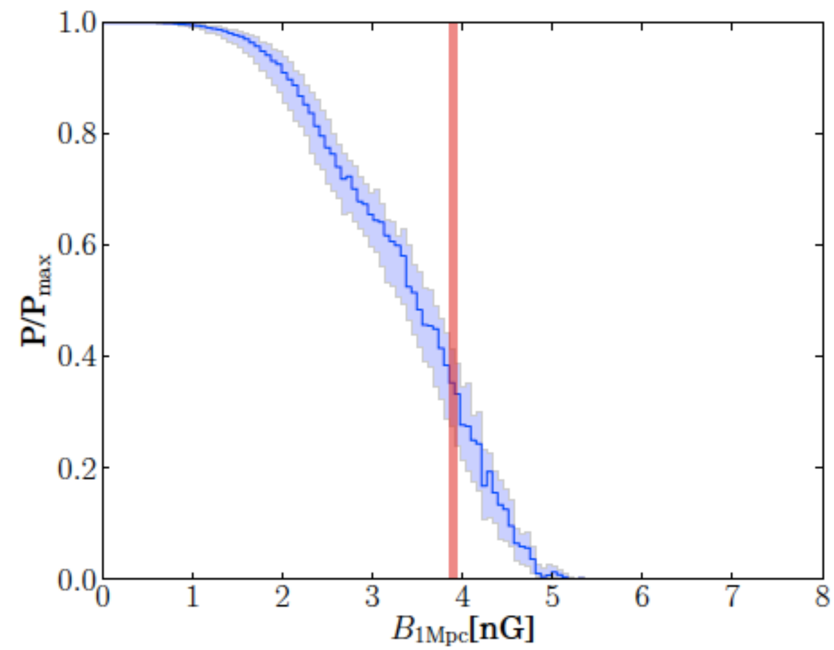

The bound on the PMF strength from the POLARBEAR CMB B-mode spectrum

B-modes from magnetic fields

- Constrain the spectrum and the epoch of PMF generation
- Magnetic stress-energy is quadratic in B

$$T^0_0 \;\propto\; -B^2$$
$$T^i_j \;\propto\; B^2\delta^i_j - 2B^iB_j$$

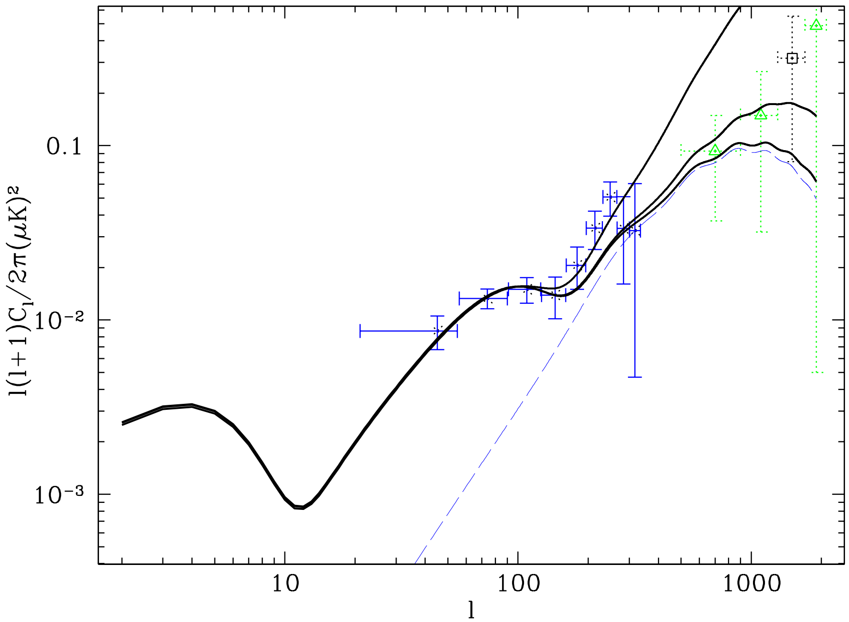

- $C_L \sim B^4$; the current bound will remain at ~nG for years to come!

Faraday Rotation is linear in B

Faraday Rotation

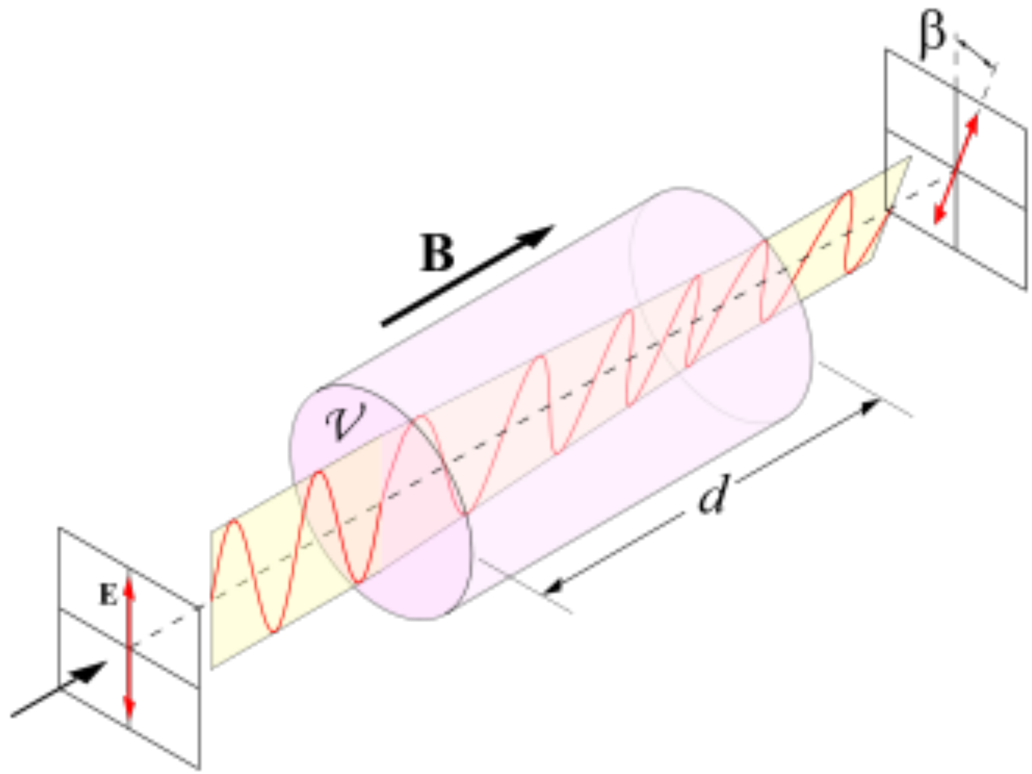

For CMB: $$\alpha(\hat{\mathbf{n}}) = \frac{3c^2\nu_0^{-2}}{16\pi^2 e}\int \dot{\tau}\ \mathbf{B}\cdot d\mathbf{l} = c^2\nu_0^{-2}\ \mathrm{RM}(\hat{\mathbf{n}})$$

Radiative transport with Faraday Rotation

$$
\begin{aligned}
\dot{Q} + i(\vec{k}\cdot\hat{n})Q &= -\dot{\tau}Q + 2\omega_B U + S_+ \\
\dot{U} + i(\vec{k}\cdot\hat{n})U &= -\dot{\tau}U - 2\omega_B Q + S_-
\end{aligned}
$$

$$
\omega_B = \frac{d\alpha}{d\eta} = \frac{3\lambda_0^2}{2\pi e}\dot{\tau}\mathbf{B}\cdot\hat{n}
$$

Instant Last Scattering Approximation

- CMB polarization is produced at last scattering ($Q^{(0)}$ and $U^{(0)}$)
- Then Faraday Rotated by a small angle

$$\alpha(\hat{\mathbf{n}}) = \frac{3c^2\nu_0^{-2}}{16\pi^2 e}\int \dot{\tau}\,\mathbf{B}\cdot d\mathbf{l} = c^2\nu_0^{-2}\ \mathrm{RM}(\hat{\mathbf{n}})$$

- We observe $Q(\nu)$ and $U(\nu)$

$$Q(\nu) + iU(\nu) = (Q^{(0)} + iU^{(0)})\exp(2i\alpha(\nu))$$

Mode-coupling correlations

- Faraday Rotation correlates multipoles of E and B in a particular way

$$B_{lm} = 2 \sum_{LM} \sum_{l'm'} \alpha_{LM} E_{l'm'} \xi^{LM}_{lml'm'} H^{L}_{ll'}$$

- Can reconstruct the rotation angle from mode-coupling EB correlations (Kamionkowski, 2009)

$$\hat{D}^{LM,\mathrm{map}}_{ll'} = \frac{4\pi}{(2l+1)(2l'+1)} \sum_{mm'} B^{\mathrm{map}}_{lm} E^{\mathrm{map}*}_{l'm'} \xi^{LM}_{lml'm'}$$

$$[\hat{\alpha}_{LM}]_{ll'} = \frac{\hat{D}^{LM,\mathrm{map}}_{ll'}}{2 C^{EE}_{l} H^{L}_{ll'}}$$

Forecasted constraints on the primordial magnetic field strength

Name - freq (GHz)	$f_{\rm sky}$ ($f_{\rm sky}^{\rm opt}$)	FWHM (arcmin)	Δ_P(μK-arcmin)	$B_{\rm eff}$ (2σ, nG)	+DL (nG)	+DL+DG (nG)
Planck LFI - 30	0.6	33	240	16^b	same	same
Planck HFI - 100	0.7	9.7	106	23	same	same
Polarbear - 90	0.024^a	6.7	7.6	3.3	3.0	same
QUIET II - 40	0.04^a	23	1.7	0.46	0.26	0.25
CMBPOL - 30	0.6	26	19	0.56	0.55	0.51
CMBPOL - 45	0.7	17	8.25	0.38	0.35	0.29
CMBPOL - 70	0.7	11	4.23	0.39	0.32	0.26
CMBPOL - 100	0.7	8	3.22	0.52	0.4	0.34
Suborbital - 30	0.1	1.3	3	0.09	0.07	0.05
Suborbital - 90	0.1	1.3	3	0.63	0.45	same
Space - 30	0.6 (0.2)	4	1.4	0.06	0.04	0.02
Space - 90	0.7 (0.4)	4	1.4	0.26	0.15	0.12

TABLE II: The expected 2σ bound in nano-Gauss on the strength of a scale-invariant PMF. Without de-lensing and with de-lensing (+DL) by a factor $f_{\rm DL} = 0.01$, and with additional removal of the galactic RM by a factor $f_{\rm DG} = 0.1$ (+DL+DG). Note that for full sky experiments, there is an optimal sky cut ($f_{\rm sky}^{\rm opt}$) that gives the best bounds on the PMF. ([a] based on 0.1 of RM sky; [b] from TB estimator.)

De, LP, Vachaspati, PRD'13, arXiv:1305.7225

- A realistic next generation CMB polarization experiment can detect a 0.1 nG scale-invariant PMF without de-lensing or subtraction of the Galactic FR

- In principle, fields of 0.01 nG and can be detected with more sensitive detectors, higher resolution, subtraction of the Galactic FR and de-lensing

Which length scales are probed?

- Most of the information comes from CMB correlations at 300 < l < 3000 (3 - 40 arcmin)
  - need high resolution polarization maps
  - can work with a small patch of sky near the Galactic poles

- Probes rotation angle correlations in the 2 < L < 100 range (scales > 1°)
  - probes PMF correlations on scales > 100 Mpc

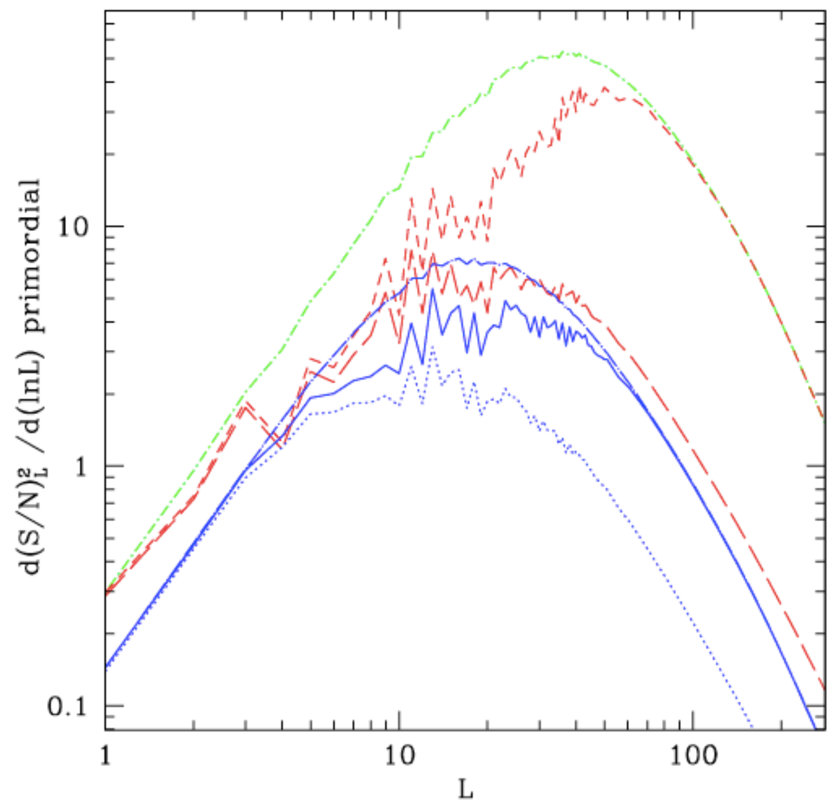

FIG. 5: Contribution of individual multipoles to the net SNR of detection of the PMF of 0.1 nG. Plotted are $d(S/N)^2_L/d\ln L$ for an optimistic 30 GHz sub-orbital experiment without de-lensing (blue dot), after de-lensing ($f_{\rm DL} = 0.01$, solid blue) and after de-lensing and partially subtracting the galactic RM (($f_{\rm DG} = 0.1$, blue long dash-dot), as well as for a hypothetical future 30 GHz space probe with (red short dash) and without (red long dash) de-lensing ($f_{\rm DL} = 0.01$), as well as with partial ($f_{\rm DG} = 0.1$) subtraction of the galactic RM (green dash-dot).

Summary

- BB can constrain PMF better than the rest of CMB spectra
- Bounds on PMF from CMB spectra will remain at ~ 1 nG
- Mode-coupling correlations induced by Faraday rotation can provide a better probe than CMB spectra

~0.01 nG vs ~1 nG

Metric perturbations and the role of neutrinos

- Before neutrino decoupling, all of the matter is tightly coupled, no fluid to balance the anisotropic stress of the PMF

  - logarithmically growing scalar and tensor modes

$$H^{(2)} \approx R_\gamma \Pi_B^{(2)} \left[\log\left(\tau_\nu/\tau_B\right) + \left(\frac{5}{8R_\nu} - 1\right) \right]$$

- After neutrino decoupling, the PMF contribution to the metric perturbations is compensated by neutrinos

Lewis (2004); Shaw and Lewis, 0911.2714

Exact *vs* Instant

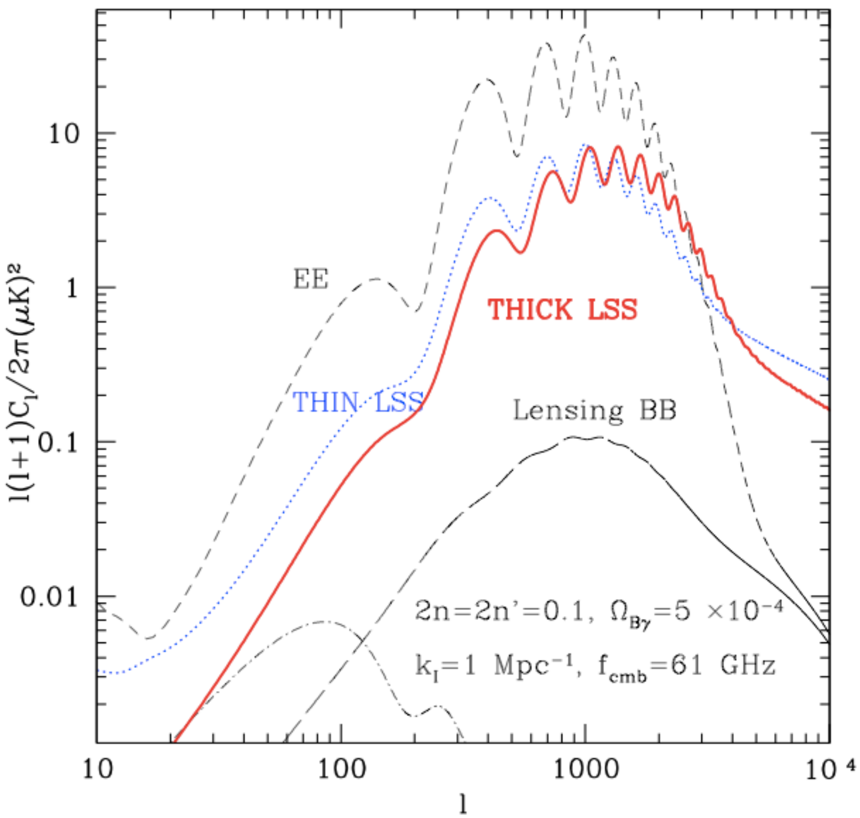

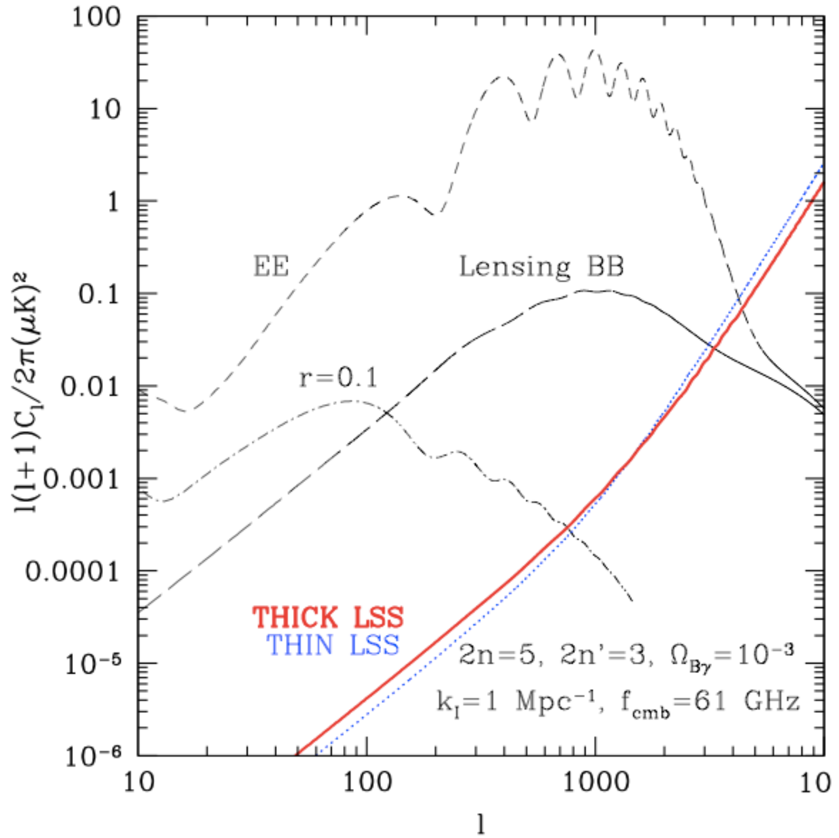

LP, Yadav, Ng, Vachaspati, PRD'11, arXiv:1106.1438

BB from Faraday Rotation @ 30GHz

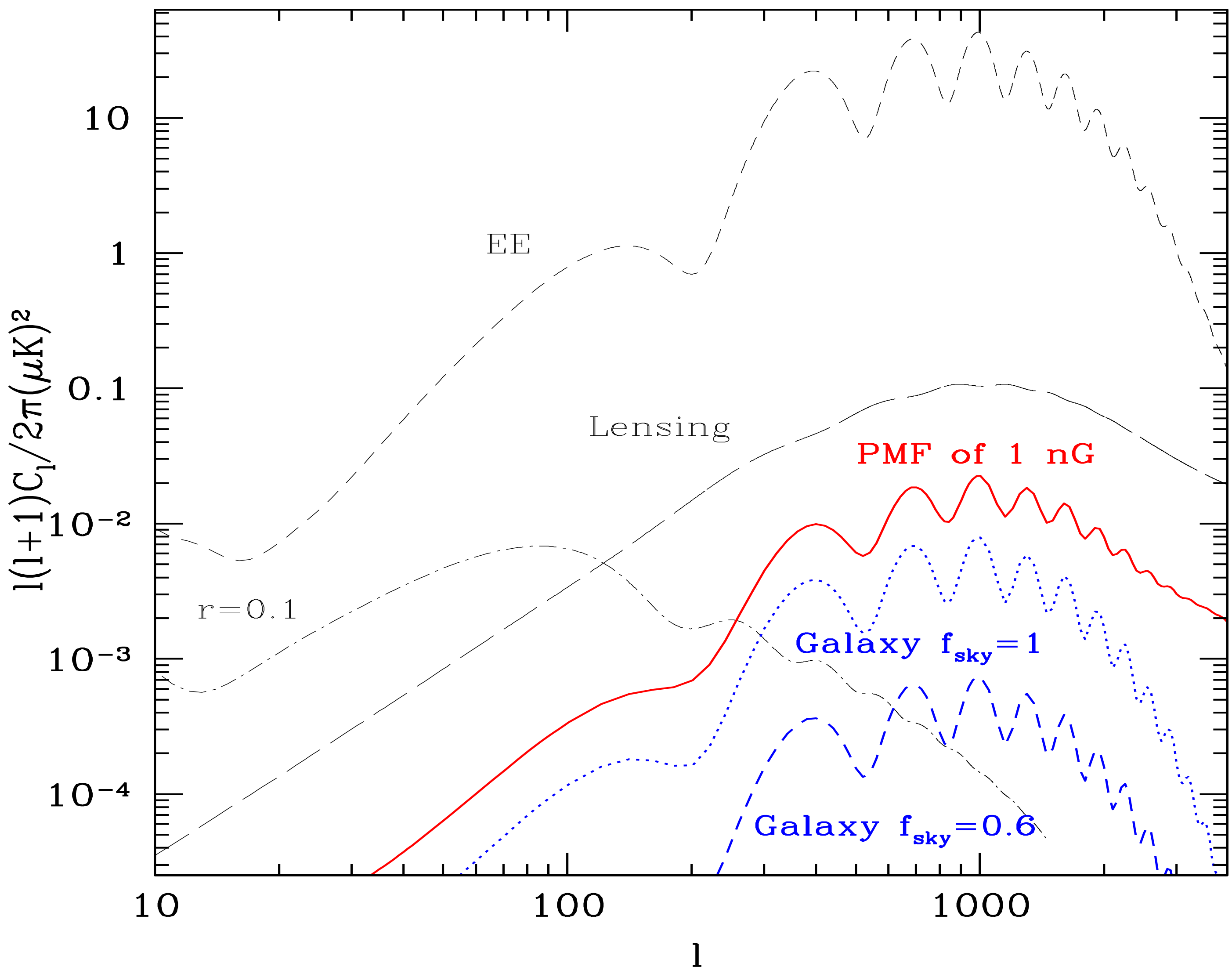

Instant Last Scattering Approximation

- Assume only E-mode polarization is produced at last scattering

$$B_{lm} = 2(-1)^m \sum_{LM} \sum_{l_2 m_2} \alpha_{LM} E_{l_2 m_2} \xi^{LM}_{lml_2m_2} H^L_{ll_2}$$

- Rotation spectrum: $\langle \alpha(\hat{n}) \alpha(\hat{n}') \rangle = \sum_L \frac{(2L+1)}{4\pi} C_L^{\alpha\alpha} P_l(\hat{n} \cdot \hat{n}')$

- Faraday Rotation contribution to the B-mode spectrum:

$$C_l^{BB} = \frac{1}{\pi} \sum_L (2L+1) C_L^{\alpha\alpha} \sum_{l_1} (2l_1+1) C_{l_1}^{EE} \, (H^L_{ll_1})^2$$

CMB Faraday rotation as seen through the Milky Way

De, LP, Vachaspati, PRD'13, arXiv:1305.7225

- Magnetic fields in our Galaxy contribute to Faraday rotation (FR) of CMB
- Galactic rotation measure estimated using extragalactic radio sources

  Oppermann et al, A&A'12, arXiv:1111.6186

- Two questions:

  1) How sensitive are CMB polarization experiments to the Galactic FR?

  2) What bounds on PMF can be placed from measurements of FR?

Galactic Rotation Measure

$$\alpha(\hat{\mathbf{n}}) = \lambda_0^2 \; RM(\hat{\mathbf{n}})$$

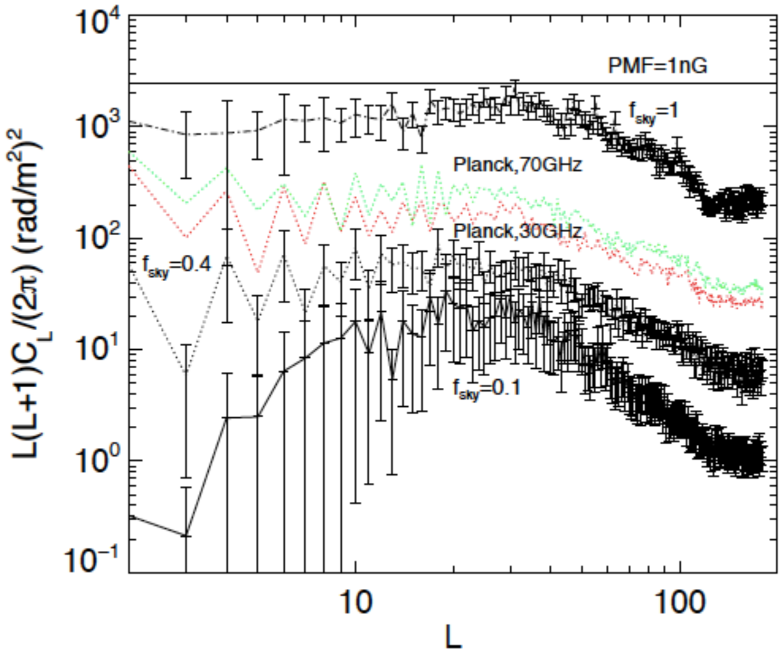

FIG. 3: The RM angular spectra, $L(L+1)C_L^{\rm RM}/2\pi$, obtained from the RM map of Oppermann et al [16] with different cuts. Shown are the RM spectra corresponding to, from top to bottom, a scale-invariant PMF of 1 nG, galaxy with no sky cut, with a mask used by Planck for their 70 GHz map, a Planck mask for the 30 GHz map, and symmetric cuts corresponding to $f_{\rm sky} = 0.4$ and $f_{\rm sky} = 0.1$.

RM in rad/m²

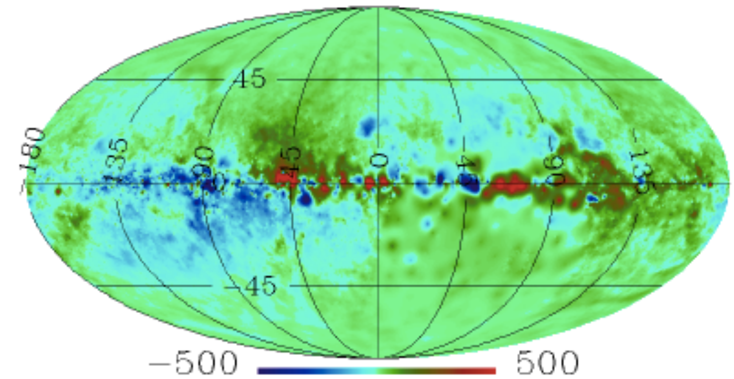

Uncertainty in RM in rad/m²

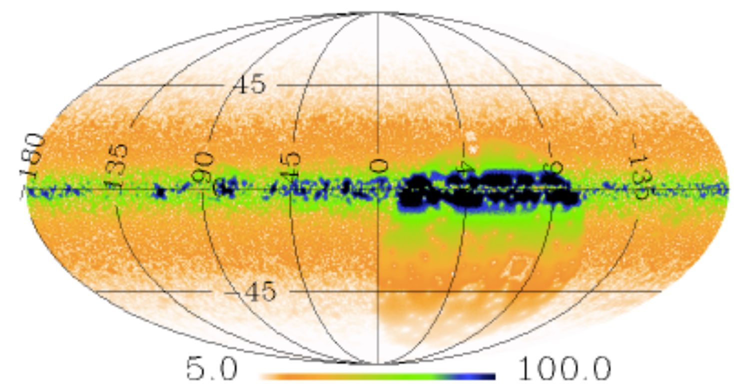

Galactic RM in rad/m² with Planck mask at 30GHz

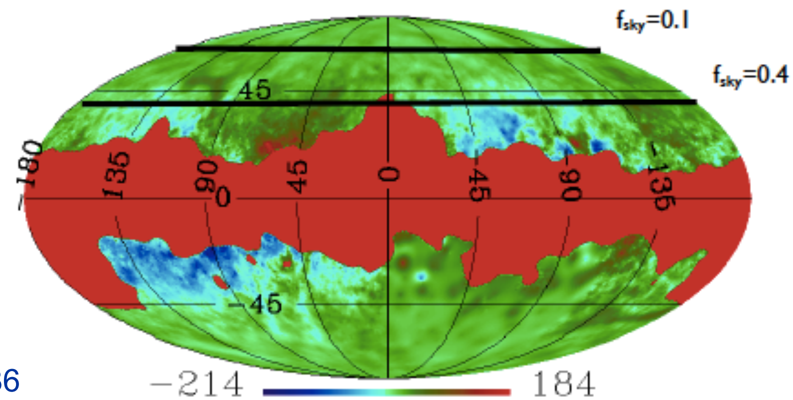

Figures from De, LP, Vachaspati, PRD'13, arXiv:1305.7225
based on the public RM data from Oppermann et al, A&A'12, arXiv:1111.6186

Forecasted signal to noise of the Galactic RM detection

Name - freq (GHz)	$f_{\rm sky}$	FWHM (arcmin)	Δ_P(μK-arcmin)	$(S/N)_{EB}$ (+DL)	$(S/N)_{TB}$ (+DL)	$(S/N)_{BB}$ (+DL)
Planck LFI - 30	0.6	33	240	5.3E-4 (same)	2.2E-3 (same)	2.3E-4 (same)
Planck HFI - 100	0.7	9.7	106	1.4E-3 (same)	7.5E-4 (same)	6E-5 (same)
Polarbear - 90	0.024[a]	6.7	7.6	1.3E-2 (1.5E-2)	1.6E-3 (2.0E-3)	4.6E-4 (6.0E-4)
QUIET II - 40	0.04[a]	23	1.7	0.3 (0.8)	0.05 (0.2)	0.02 (0.08)
CMBPOL - 30	0.6	26	19	1.0 (same)	0.4 (same)	0.05 (same)
CMBPOL - 45	0.7	17	8.25	2.1 (2.3)	0.8 (0.9)	0.12 (0.15)
CMBPOL - 70	0.7	11	4.23	2.0 (2.6)	0.6 (0.9)	0.08 (0.14)
CMBPOL - 100	0.7	8	3.22	1.4 (2.0)	0.3 (0.6)	0.03 (0.07)
Suborbital - 30	0.1	1.3	3	2.0 (3.1)	0.3 (0.7)	0.08 (0.2)
Space - 30	0.6	4	1.4	18 (28)	7 (14)	5 (30)
Space - 90	0.7	4	1.4	3.3 (6.8)	1.0 (2.4)	0.09 (0.64)

TABLE I: S/N of the overall detection of the galactic RM spectrum with Planck, Polarbear, QUIET, CMBPOL and optimistic future sub-orbital and space experiments. Results are presented without and with (+DL) de-lensing by a factor $f_{\rm DL} = 0.01$. ([a] based on 0.1 of RM sky.)

De, LP, Vachaspati, PRD'13, arXiv:1305.7225

- The Galactic contribution to Faraday Rotation is negligible today but will be detectable with the next generation of CMB polarization experiments
- It will obscure the FR signal from recombination

Dependence on detector noise and resolution

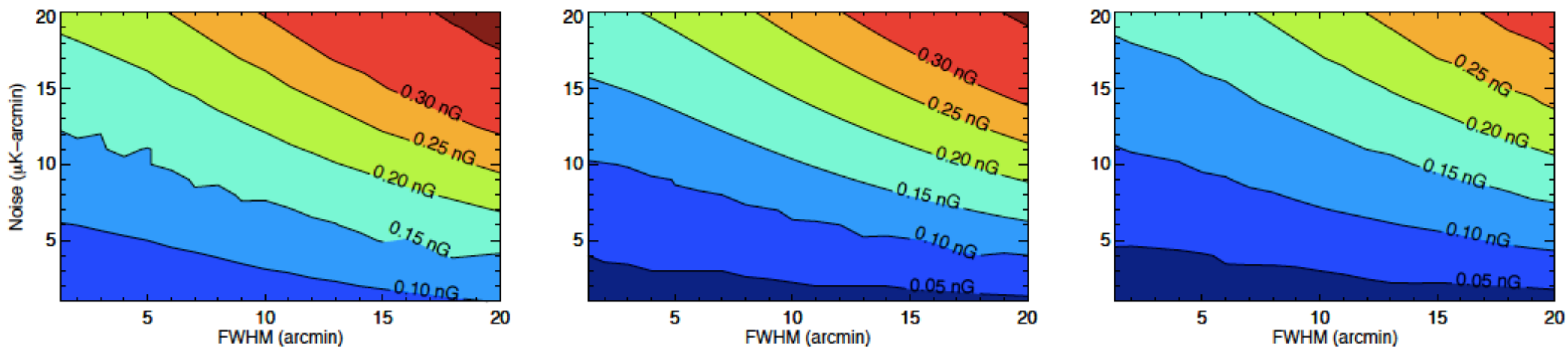

FIG. 6: Contour plots of the 2σ bound on $B_{\rm eff}$ (in nG) in the instrumental noise – CMB resolution plane, with the frequency channel taken to be 30 GHz. The left panel shows the case with no de-lensing ($f_{\rm DL} = 1$) and without subtracting the Milky Way RM ($f_{\rm DG} = 1$). The middle panel is with $f_{\rm DL} = 0.01$, while the right panel is with $f_{\rm DL} = 0.01$ and $f_{\rm DG} = 0.1$. It is assumed that up to 0.6 of the sky is available and an optimal sky cut is found in each case.

De, LP, Vachaspati, PRD'13, arXiv:1305.7225

If $C_L^{RM} > \sigma_L$ for some L (signal dominated), then

$$\frac{S}{N} \approx \left(28 - \frac{\theta^i_{\rm fwhm}}{\theta^1_{\rm fwhm}}\right)\left(\frac{B_{\rm SI}}{0.1{\rm nG}}\right)\left(\frac{30{\rm GHz}}{\nu_i}\right)^2 \frac{\sigma_{P,1}}{\sigma_{P,i}}$$

Otherwise,

$$\left(\frac{S}{N}\right)^2 = \sum_{L=1}^{L_{max}} \frac{(f_{\rm sky}/2)(2L+1)[C_L^{\rm RM,PMF}]^2}{[C_L^{\rm RM,PMF} + f_{\rm DG} C_L^{\rm RM,G} + \sigma^2_{{\rm RM},L}]^2}$$

LP, MNRAS'14, arXiv:1311.2926

Combining multiple frequencies

$$[\hat{r}_{B^i E^j,LM}]_{ll'} = c^{-2}\nu_i^2[\hat{\alpha}_{B^i E^j,LM}]_{ll'}$$

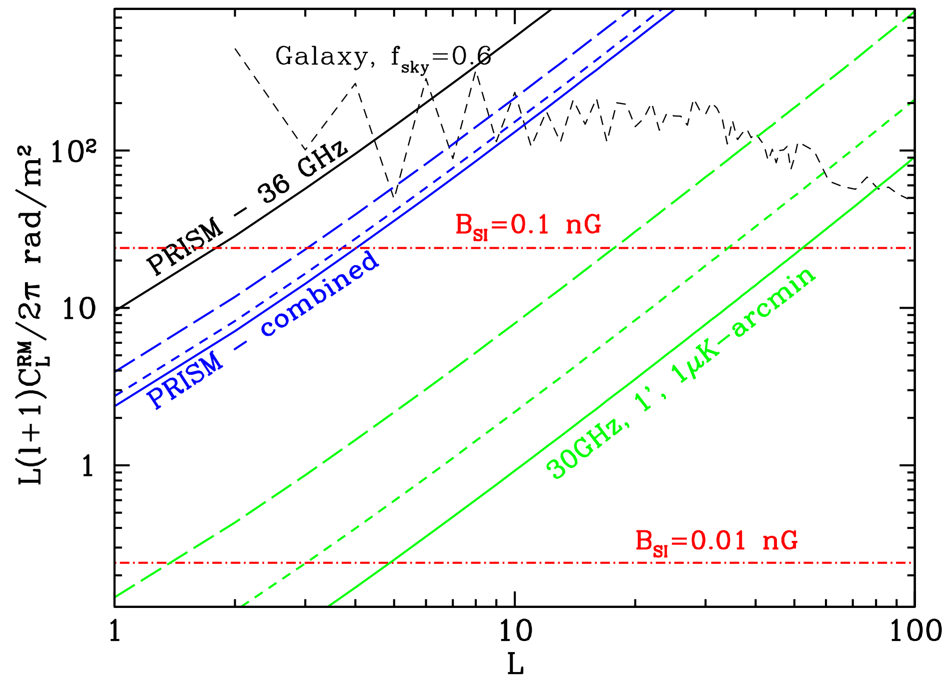

S/N of detection (by PRISM) of a 0.1 nG strength scale-invariant PMF

ν (GHz)	$\theta_{\rm fwhm}$	$\sigma_P(\mu$K-arcmin)	$(S/N)^{f_{\rm DL}=0}_{f_{\rm DG}=0}$	$(S/N)^{f_{\rm DL}=1}_{f_{\rm DG}=0}$	$(S/N)^{f_{\rm DL}=0}_{f_{\rm DG}=0.1}$
30	17′	13	0.75	0.7	0.6
36	14′	8.5	1	0.9	0.85
43	12′	8	0.78	0.68	0.66
51	10′	6.2	0.82	0.72	0.67
62	8.2′	6	0.57	0.45	0.5
75	6.8′	5.6	0.4	0.3	0.34
90	5.7′	5.4	0.24	0.18	0.22
all	-	-	2.4	1.95	1.9

LP, MNRAS'14, arXiv:1311.2926